A non-olfactory shark adenosine receptor activates CFTR with unique pharmacology and structural features

Sumeet Bhanot, Gabriele Hemminger, Stephen G. Aller and John N. Forrest Jr.

Renal Section, Department of Medicine, Yale University School of Medicine, New Haven CT 06510
The Mount Desert Island Biological Laboratory, Salisbury Cove, ME 04672
The Department of Pharmacology & Toxicology, University of Alabama at Birmingham, Birmingham, AL 35205

Running Head: Characterization of a novel adenosine receptor (A_0) from the shark rectal gland (*Squalus acanthias*)

Corresponding Authors: Stephen G. Aller, Department of Pharmacology & Toxicology, University of Birmingham at Alabama, Birmingham, AL 35205, sgaller@uab.edu
and John N. Forrest Jr., Department of Medicine, Yale University School of Medicine, 367 Cedar St., New Haven CT 06510, john.forrest@yale.edu

Abstract

Adenosine receptors (ADORs) are G-protein coupled purinoceptors that have several functions including regulation of chloride secretion via CFTR in human airway and kidney. We cloned an ADOR from *Squalus acanthias* (shark) that likely regulates CFTR in the rectal gland. Phylogenic- and expression- analyses indicate that elasmobranch ADORs are non-olfactory, and appear to represent extant predecessors of mammalian ADORs. We therefore designate the shark ADOR as the A_0 receptor. We co-expressed A_0 with CFTR in *Xenopus laevis* oocytes and characterized the coupling of A_0 to the chloride channel. Two electrode voltage clamping was performed and current-voltage (I-V) responses were recorded to monitor CFTR status. Only in A_0- and CFTR- co-injected oocytes did adenosine analogs produce a significant dose-dependent activation of CFTR consistent with its electrophysiological signature. A pharmacological profile for A_0 was obtained for ADOR agonists and antagonists that differed markedly from all mammalian ADOR subtypes (agonists: R-PIA > S-PIA > CGS21680 > CPA > 2ClADO > CV1808 = DPMA > NECA) and (antagonists: DPCPX > PD115199 > 8PT > CGC > CGS15943). Structures of human ADORs permitted a high-confidence homology model of the shark A_0 core which revealed unique structural features of ancestral receptors. We conclude: (1) A_0 is a novel and unique adenosine receptor ancestor by functional and structural criteria; (2) A_0 likely activates CFTR *in vivo* and this receptor activates CFTR in oocytes indicating an evolutionary coupling between ADORs and chloride secretion; and (3) A_0 appears to be a non-olfactory evolutionary ancestor of all four mammalian ADOR subtypes.

Keywords

Adenosine receptor, molecular evolution, shark, structural biology, CFTR, chloride secretion

Significance Statement

We have cloned and characterized an ancient adenosine receptor from sharks that is unlikely to be olfactory in function. The shark receptor, which we designate as A_0, has a unique pharmacological profile, characteristic structural features, and is also highly likely to be the dominant ADOR regulator of the shark ancient ortholog of the Cystic Fibrosis chloride channel, called CFTR.

Introduction

The ubiquitous nucleoside adenosine exhibits broad importance by providing a structural basis for cellular energy storage in the form of ATP, contributing to the structural make-up of the genetic code in both DNA and RNA, and modulating a multitude of receptor mediated physiological functions. Adenosine itself is therefore an early ancestral building block in the biochemistry of life on Earth.

Two broad classes of purinoceptors, P_1 & P_2, recognize and bind adenosine-based nucleosides and nucleotides, and can be distinguished by two anti-parallel pharmacological profiles (P_1: Adenosine > AMP > ADP > ATP & P_2: ATP > ADP > AMP > Adenosine) (1). Receptors specific for adenosine (ADORs) are divided into four non-olfactory subtypes including A_1, A_{2a}, A_{2b} & A_3, which couple to $G_{o,i(1-3)}$, G_s, G_s and $G_{i(2,3),q\text{-like}}$ G proteins, respectively (2-7). Typically, all ADORs modulate the activity of at least one of a number of different isoforms of adenylate cyclase through the coupling to a G protein. The A_1 ADOR can also modulate other effector systems, namely potassium channels, calcium channels, phospholipase A and C (7).

One major unifying theme in the function of ADORs in mammals appears to be a feedback mechanism to either curb metabolic activity of the cell or to oppositely vasodilate for increasing oxygen supply and meet higher metabolic demand (8). Relatedly, in sharks, which evolved prior to any land-based vertebrate, low concentrations of adenosine released from metabolic activity by the highly active shark rectal gland of *Squalus acanthias*, serve as an autocoid feedback inhibitor to slow ion transport (9). Curiously, high concentrations of adenosine (~10 μM) increased ion transport activity at both the apical- and basolateral-membranes, and stimulated chloride secretion in rectal gland via the shark ortholog of the Cystic Fibrosis transmembrane Conductance Regulator (CFTR) (10,11). Shark CFTR is an impressive 70% identical to human CFTR at the amino acid residue sequence level (12), and an ancient evolutionary link in ADOR signaling of CFTR activity in both fish and mammals is now well established.

The four main ADOR subtypes (A_1, A_{2a}, A_{2b} & A_3), first identified in many different mammals and now observed in the genomes of birds, reptiles, amphibians and fish, can be distinguished at phylogenetic- and pharmacological levels. For the A_1 receptor, the adenosine analogs CPA and R-PIA are the most potent, while CV1808 and CGS21680 are weaker agonists. For A_{2a}, NECA, CV1808, and CGS21680 are the most potent agonists, and CPA is less potent. The A_{2b} receptor subtype responds with high potency to NECA but exhibits little or no response to CV1808 and CGS21680. A fifth ADOR subtype, designated A2c, was more recently identified and was shown to be an olfactory ADOR that allows fish to sense adenosine released into the water by potential prey (13).

We sought to examine ADORs in *Squalus acanthias* and we identified a single receptor with highest expression in the rectal gland and stomach, but very low levels in brain and other tissues. Phylogenetic analysis shows that the *Squalus acanthias* ADOR, as well as putative ADORs identified by genome sequencing from other sharks, amphibians and reptiles, form a separate clade that is distinct from the other five ADOR subtypes. We used the *Xenopus laevis* oocyte system to co-express the *Squalus acanthias* ADOR with CFTR to demonstrate the coupling of receptor to chloride channel. Co-injected oocytes revealed a pharmacological profile of *Squalus acanthias* ADOR that is unique from all four major subtypes of ADORs. We argue that the *Squalus acanthias* ADOR is not olfactory and that the clade containing the elasmobranch ADORs is ancestral to the four major subtypes. We therefore designated the shark ADOR as A_0-ADOR, and characterize this ancestral receptor here including novel structural features revealed by three-dimensional atomic homology modeling.

Materials and Methods

Molecular Biology

Details describing the molecular biology (preparation of total RNA from shark tissue, degenerate PCR, library screening, RACE PCR, Northern blot, qRT-PCR and electrophysiology in oocytes) are presented in the supplementary material (see supplementary figs. S1-S5). Human CFTR was obtained from Dr. Carol Semrad in the pKS-βglobin-CFTR-polyAC plasmid and human adenosine receptors were provided by Dr. Joel Linden. Capped messenger RNA for all receptors was synthesized from linearized plasmid templates using the Ambion mMessage mMachine T7 *in vitro* transcription kit according to the manufacturer's protocol.

To retrieve putative adenosine receptor coding sequences with good representation from mammals, birds, reptiles, amphibians and fish, multiple database searches were carried out using the NCBI BlastP Server against the full nonredundant dataset. To find potential ancestral receptor sequences, additional searches using shark A_0 sequence were performed excluding the Mammalia taxid (40674). Global alignments were performed using the Clustal method (14) within the Lasergene software package (DNASTAR, Inc) and similar results were obtained using the implementation of Clustal Omega (15) in the EMBOSS package (16) and standard parameters (17). Alignments for phylogenetic analyses including the production of the phylogenetic tree in figure 1 were conducted with MEGA7 (18).

Xenopus laevis expression system

Adult female *Xenopus laevis* were obtained from Nasco and Xenopus 1, and housed in the animal care facilities at Yale University. Surgeries to harvest oocytes were performed 4-7 days prior to experiments according to a protocol approved by the Yale Animal Care Committee. Injection pipets pulled on a Sachs-Flaming Micropipette puller-Model PC-84, using Drummond 210/310/510 glass pipettes were beveled to a tip diameter of 10-15 µm. The pipettes were back-filled with mineral oil and attached to a Drummond microinjector, in preparation for cRNA aspiration and oocyte injection. Oocytes were injected with 50 nl (~15 ng) of cRNA encoding shark A_0- or human A_1, A_{2a}, A_{2b}, or A_3 receptors and 5-10 ng of human CFTR, and subsequently incubated for 3-5 days at 18-20 °C before experiments.

Oocytes were prepared for two electrode voltage clamping by inserting two 0.6-0.9 MΩ, 3 M KCl filled Ag electrodes, pulled on a Sachs-Flaming micro-pipet puller model PC-84, using borosilicated glass obtained from Sutter Instrument (BF120-69-10). Oocytes were perifused with frog Ringer's (98 mM NaCl, 2 mM KCl, 1.8 mM $CaCl_2$, 1 mM $MgCl_2$ and 5 mM HEPES. Adjusted to pH 7.4), which was also used in the preparation of solutions for the pharmacological agents tested. Oocytes were voltage clamped using the Dagan TEV-200 amplifier along with the Dagan LM-12 Lab Interface, on a PC computer running pClamp Version 5.5 software. The Soltec 1242 plotter was used to acquire the data. Oocytes were clamped at -60 mV and the current was measured as a function of time. Moreover, frequent voltage pulses (-120mV to +60mV) were performed to determine the current-voltage (I-V) relationship at any given timepoint. Data were corrected for any capacitive current incurred due to the voltage pulses. Weak data were obtained with the human A_{2a} and A_3 receptors, which presumably do not couple efficiently to frog G proteins or the proper adenylate cyclase(s) for CFTR activation, and were omitted from the analysis.

Data analysis was performed using Microsoft Excel. Some of the data were analyzed using an Excel macro provided by the lab of Dr. David Dawson, which allowed the subtraction of the capacitive current from the current voltage relationship, incurred during the voltage pulses. Statistical analysis was

limited to standard error of the mean performed on the dose response of the shark A_0 receptor. Supplementary fig. S6 illustrates the two-electrode voltage clamping set-up for expression studies in *Xenopus* oocytes.

Homology model of the shark A_0

At the time of this writing there were 48 high-resolution structures of adenosine receptors in the Protein Data Bank (PDB) as determined by either x-ray crystallography or cryo-electron microscopy. All structures are human in origin and only two of the four known subtypes were represented, A_{2a} (n=45) and A_1 (n=3). We chose a small subset for consideration as templates for homology modeling of the shark A_0 receptor: A_{2a} with adenosine bound (PDB code 2ydv) (19), A_1 with adenosine (6d9h) (20), A_{2a} with N-ethyl-5'-carboxamido adenosine, NECA (6gdg) (21), and A_{2a} with CGS21680 (4ug2) (22). Primary amino acid sequence alignments between shark A_0 sequence and the selected subset were performed using NCBI Cobalt (23). Amino acid sequences present in the human receptors but not present in shark A_0 were removed (see full alignment between shark A_0 and human A_{2a} in supplementary fig. S7). The human A_{2a} receptor appeared to be a sufficiently good template for A_0 modeling as it shares 45% identical amino acid sequence with A_0 and exhibited an NCBI Cobalt 3-bit amino acid chemical similarity of 81% after removing disordered sequences from the A_{2a} structure, and after removing sequences present in either receptor but not the other (supplementary fig S8). Using the A_{2a} x-ray crystal structure template (PDB code 2ydv), A_{2a} insertion sequences were removed and mutagenesis to A_0 was performed with scripts written in perl and PyMOL version 2.0.6 (Schrödinger, LLC). Two short amino acid sequences of shark A_0 that are not present in the human receptors (i.e. A_0-Arg95 and A_0-Asn228-Ser230), were inserted into the 3-dimensional model using Coot version 0.8.9 (24) and model minimization/regularization. Refinements using phenix (25) of A_0 against A_{2a} dataset (PDB code 2ydv) were performed by replacing the human receptor with the shark starting model. Three rounds of rigid body, XYZ-reciprocal space and B-factor refinement were performed including secondary-structure restrains and Ramachandran/rotamer optimization, all with resolution cutoff set to 4.0 Å resolution. Parameterization of the R-PIA ligand was accomplished using phenix (25) starting with the Simplified Molecular-Input Line-Entry System (SMILES) string for the ligand (26): C[C@H](Cc1ccccc1)Nc2ncnc3n(cnc23)[C@@H]4O[C@H](CO)[C@@H](O)[C@H]4O
The position of the lipid bilayer was predicted based on the location of conserved aromatic amino acids known to interact with lipid head groups spaced ~35 Å apart (27).

Results

Identification of shark A_0 ADOR

Since the *Squalus acanthias* genome is not yet available and there is some uncertainty associated with the search for *bona fide* protein-coding sequences from genomic data, we sought to clone shark adenosine receptors using reverse-transcription procedures from mRNA/cDNA prepared from shark tissues. PCR of shark rectal gland cDNA using degenerate primers to conserved regions of transmembrane domains 5 and 7 of previously cloned ADORs yielded a single 352 bp product (see supplementary fig. S1). The translated amino acid sequence of this fragment (P-SH12) had highest homology to ADORs that was only 39-45% identical to the human receptor sub-types (A_1, A_{2a}, A_{2b} and A_3). Northern blot and quantitative RT-PCR (qRT-PCR) revealed strongest expression of the putative shark ADOR in the rectal gland and stomach with weak levels in other tissues including the brain (supplementary figs. S2 and S3). To control for the quality of cDNA template used in the qRT-

191 PCR experiments, shark CFTR was amplified from the same cDNA templates prepared from the various
192 shark tissues. Results showed abundant CFTR expression in rectal gland, intestine, brain and testis
193 (supplementary fig. S4).
194 Screening of a shark rectal gland cDNA library using ^{32}P-labeled P-SH12 yielded more
195 nucleotide sequence from a single putative ADOR and allowed the design of primers for Rapid
196 Amplification of cDNA Ends-PCR (RACE-PCR). Extensive rounds of both cDNA library screening and
197 RACE-PCR using total RNA from shark rectal gland revealed only a single putative ADOR entity
198 which we designate here as the shark A_0 receptor (for details see supplementary material).
199 Hydropathy analysis of the putative shark A_0 ADOR amino acid sequence revealed seven
200 predicted transmembrane regions and a predicted extracellular orientation of the N-terminus that was
201 consistent with all known G protein-coupled receptors (see supplementary fig. S5). Phylogenetic
202 analysis of known- and putative- ADORs revealed an ancestral branch that included dogfish shark A_0
203 and other putative ADORs from non-mammalian species that are distinct from the recently discovered
204 olfactory ADORs (Wakisaka et al. 2017; figure 1). Ancestral olfactory- and non-olfactory receptors
205 could be distinguished from the four specialized mammalian subtypes (i.e. A_1, A_{2a}, A_{2b} and A_3) as
206 having an abbreviated second extracellular loop (ECL2) at 9 amino acid (aa) residues (supplementary
207 fig. S9). ECL2 of A_1 is elongated by 4-17 aa (n=42 receptor species examined), ECL2 of A_{2a} is
208 elongated by 8-14 aa (n=22), ECL2 of A_{2b} is elongated by 10-19 aa (n=28) and ECL2 of A_3 is
209 elongated by 1-7 aa (n=18, see supplementary fig. S10). Assuming mutagenesis rates of all adenosine
210 receptors are similar amongst species, we interpret the phylogram to indicate that the elasmobranch A_0
211 ADOR belongs to an evolutionary ancestral branch of the specialized adenosine receptor subtypes. We
212 next surmised that shark A_0 is responsive to adenosine analogs with potentially unique properties
213 compared to known receptor subtypes, and we sought to test this hypothesis using functional and
214 pharmacological characterization in *Xenopus laevis* oocytes.
215
216 **CFTR expression**
217 Expression studies were conducted in oocytes co-injected with human CFTR and shark A_0
218 cRNA, and current-voltage (I-V) relationships were determined by conducting voltage pulses (-120 mV
219 to +60 mV) and measuring the clamping current. Expression of CFTR was determined by the use of
220 forskolin, a well-known activator of adenylate cyclase that increases intracellular cAMP levels and
221 activates CFTR by phosphorylation of the R-domain by a cAMP dependent protein kinase A (Dulhanty
222 and Riordan 1994). Figure 2 illustrates the I-V relationships of a single representative experiment on an
223 oocyte 3 days after co-injection. Addition of 5 μM forskolin produced an increase in conductance
224 (increase in the slope of the I-V relationship) from the basal level, a decrease in the clamping current at -
225 60 mV from -76 nA to -560 nA, and a rightward shift in the reversal potential to -29.4 ± 0.43 mV (n=3
226 I-V ramps ± SEM) from a basal value of -38.0 ± 1.7 mV (n=5 ramps ± SEM). This negative,
227 non-rectifying current with a reversal potential close to that of Cl^- (Cl^-_{rev} = ~ -30 mV) has the
228 electrophysiological characteristics of a CFTR Cl^- current. Furthermore, this response was sensitive to
229 300 μM glibenclamide, an inhibitor of the CFTR Cl^- channel (28) (n=1, data not shown). The response
230 to forskolin was also inhibited by the PKA antagonist H-89 (25 μM, n=3) in oocytes injected with
231 human CFTR cRNA (data not shown), suggesting that CFTR is activated by a cAMP dependent protein
232 kinase A (PKA) in this system. The negative, non-rectifying CFTR current was absent in un-injected-
233 and water injected- oocytes (n=4) under identical conditions, and were reproducible both in the same
234 oocyte and in all oocytes injected with human CFTR cRNA. These data established expression of CFTR
235 in our system.

236 Addition of 10 μM 2-chloroadenosine in the representative oocyte (figure 2) also
237 produced an increase in total conductance by a similar non-rectifying negative current of the
238 magnitude ~ -500 nA and a reversal potential from -39.0 ± 1.7 mV (n=5 I-V ramps ± SEM) to
239 approximately -30.5 ± 0.14 mV (n=3 ramps ± SEM). This response was reversibly inhibited by
240 10 μM DPCPX, an adenosine receptor antagonist, where the clamping current at -60 mV was ~
241 -90 nA with a reversal potential of -39.4 ± 2.8 mV (n=3 ramps ± SEM), both of which are
242 reminiscent of the basal state (figure 2). This response suggested that the expression and
243 stimulation of the shark A_0 receptor is associated with an increase in Cl^- current which has
244 characteristics consistent with CFTR $C1^-$ currents. Our results also established a coupling of the
245 shark A_0 adenosine receptor and human CFTR in the *Xenopus* oocyte expression system.
246
247 **Pharmacological characterization of shark A_0**
248 Determination of the pharmacological profiles of adenosine receptor agonists and
249 antagonists in the oocyte necessitated the development of protocols in the *Xenopus laevis* oocyte
250 expression system. We first compared three agonists in a series of identical experiments to provide
251 quantitative data for statistical analysis. We then developed a second protocol to determine a
252 relative response to a larger number of agonists and antagonists to provide a more comprehensive
253 profile for comparison with other receptor profiles in the literature.
254
255 **<u>Quantitative dose response to agonists</u>**
256 Based on preliminary data, NECA, 2-chloroadenosine (2ClAdo) and R-PIA were selected to
257 determine potency order in a quantitative manner. The dose response to each agonist was measured
258 using the experimental setup depicted in figure 3. The oocyte is first stimulated with 5 μM
259 forskolin, and subsequently brought to a basal state with frog Ringer's (FR). Next the oocyte is
260 exposed to increasing doses of NECA (0.01 μM, 0.1 μM, 1 μM & 10 μM), each incremental dose
261 of the agonist was added once the response to the prior dose had peaked (n=3). This sequence was
262 followed by an identical protocol for 2-chloroadenosine (n=3) (also figure 3) and R-PIA (n=6) (not
263 shown). Variation in the sequence of the agonists tested gave similar results.
264 The initial 5μM forskolin response was used as an internal control (comparison of the
265 agonist response to forskolin) in these studies because of the variability of the expression of CFTR
266 secondary to imprecision in injection of RNA, inter-oocyte variability in CFTR expression and
267 inter-frog and intra- frog variability in the quality of the oocytes due to environmental factors. Data
268 were normalized to the response to 5μM forskolin preceding each doseresponse.
269 The data from these dose response experiments are summarized in figure 4. The peak
270 stimulation of the control oocytes (injected with human CFTR cRNA only) at 10 μM of NECA, 2-
271 chloroadenosine and R-PIA are -0.01%, 0.04% and 0.03% respectively (data normalized to 5 μM
272 forskolin response, mean=564 nA), showing very poor coupling of any endogenous oocyte
273 adenosine receptor to human CFTR. The responses of oocytes injected with human CFTR and
274 shark A_0 cRNA, at concentrations of 0.01 μM of NECA, 2-chloroadenosine and R-PIA, and 0.1
275 μM NECA and 2-chloroadenosine were not significantly different from un-injected controls
276 ($p>0.05$). The response to R-PIA at 0.1 μM (55.6%) was greater than NECA and 2-chloroadenosine
277 (2.7% and 4.2% respectively). At an agonist concentration of 1 μM the differences between the
278 three agonists NECA, 2-chloroadenosine and R-PIA (13.0%, 35.1% and 196%, respectively) were
279 appreciable and significant ($p<0.05$). The response at 10 μM (66.5%, 151% and 210% respectively)

were markedly different ($p<0.05$). These data established the potency order of R-PIA>2- chloro-adenosine>NECA for the shark A_0 adenosine receptor in *Xenopus laevis* oocytes.

Qualitative profile for agonists and antagonists

With the above profile established for the three agonists, a more extensive profile was ascertained for 8 agonists (NECA, DPMA, CV1808, 2-chloroadenosine, CPA, S-PIA, CGS21680, R-PIA) and 5 antagonists (CSC, 8PT, DPCPX, CGS15943, PD115199) to allow comparison with profiles established for the presently cloned adenosine receptors. The analysis was carried out at an agonist concentration of 1 μM and an antagonist concentration of 10 μM to optimize the analysis.

The protocol required oocyte perifusion with one agonist at 1 μM and substitution with a second after stabilization of the signal. The responses were judged as either an increase, a decrease or equivocal. The data were compiled into the agonist profile for the shark A_0 receptor of R-PIA>S-PIA>CGS21680>CPA>2-chloroadenosine>CV1808=DPMA >NECA (n=7). Varying the order of agonists produced identical results, in that the profiles conducted in order of increasing agonist potency were no different from profiles conducted in order of decreasing agonist potency.

The antagonist order of potency was carried out using a similar protocol. Oocytes were perifused with 1 μM R-PIA to generate a stable stimulated state, followed by perifusion with 1 μM R-PIA and 10 μM of the various antagonists. The antagonist profile obtained for the shark A_0 receptor was DPCPX>PD115199>8PT>CSC>CGS15943 (n=5). The relative potency order of agonists- and antagonists- were determined qualitatively in 10 different oocytes including 186 pairwise comparisons (please see supplementary tables S3).

Protocol validation using human ADORs

The human A_1, A_{2a}, A_{2b} and A_3, obtained from the Linden lab at the University of Virginia, were also examined in our oocyte system using the qualitative protocol to provide validation for this form of analysis. Although four human ADORs were expressed in the oocyte, reproducible profiles were obtained for two receptors, the human A_1 (agonist profile, n=3) and human A_{2b} (agonist profile, n=4, antagonist profile, n=3) (table 1). The human A_1 and A_{2b} receptor agonist profiles determined in oocytes are in excellent agreement with binding studies and functional studies (see supplementary table S4). However, the A_{2b} antagonist profile shows an apparent discrepancy in the potency order of CGS15943 and 8PT. This difference may be attributable to a cross species comparison (rat vs human). Taken together, this data provides strong support for the validity of our protocols used in pharmacological characterization of human- and shark- ADORs.

Homology model of shark A_0

Given the reasonable sequence homology of shark A_0 between ADORs that have been well-characterized and for which structures are known (supplementary fig. S11), we conducted exploratory refinements of the A_0 starting homology model against the deposited structure factors of the human A_{2a} x-ray crystal structure (PDB 2ydv), replacing the coordinates of A_{2a} with A_0. Refinement was restricted to low-resolution (4.0 Å) to effectively down-weight the contribution of mis-matched side chain sequences between the two species while providing a data-driven constraint for backbone atoms and secondary structure. The resulting model exhibited good protein Ramachandran- and side chain rotameric geometry (supplementary table S5) and had convincing secondary structure for the transmembrane helices and extramembrane segments (figure 5). Both

325 sequence alignments and the shark A_0 homology model revealed an abbreviated extracellular loop
326 2 (ECL2) in ancestral receptors compared to the more specialized subtypes. While it is not yet
327 known what, if any, functional consequence arises from different lengths of the ECL2 specifically,
328 more than 30 ancestral receptors in the database have a minimized ECL2 (supplementary fig. S9).
329 Thus, it would seem that ECL2 of ancestral receptors is at the minimum length necessary to
330 maintain the structure and/or function of the adenosine receptor architecture.
331
332 **Conserved Ligand-Receptor Interactions**
333 To explore the extent to which our homology model recapitulates known fundamental
334 interactions between ligand and receptor, we separately modeled adenosine (ADO), 2-
335 chloroadenosine and the most potent ligand in this work, R-phenyl-isopropyl adenosine (R-PIA),
336 into the A_0 binding pocket, conducted refinements and inspected the receptor-ligand interactions.
337 While we recognize there will be error in the process of homology modeling A_0 in the absence of
338 an actual structure, potential fundamental interactions between A_0 and ligands are well conserved
339 in the refined A_0 model compared to human ADOR structures (figure 6 and supplementary table
340 S6).
341 Among the most important known interactions between receptor and ligand occur between
342 ADOR and the purine pharmacophore of adenosine- and adenosine analogs. The structures of
343 human A_{2a}- and A_1 reveal that an aromatic residue (F168 and F171, respectively), protrudes down
344 into the ligand binding pocket and contribute an intimate π-π stacking interaction with the purine
345 ring of adenosine (29). Our refined homology model of shark preserves this interaction
346 convincingly well, with the corresponding A_0 aromatic residue being F179 (figure 6). A second
347 critical interaction revealed by the structures of A_{2a}- and A_1 is a strong polar interaction, most
348 likely hydrogen bonding, between an asparagine residue (N253 and N254, respectively) and the N7
349 nitrogen and the amino group of C6 of the purine ring. The corresponding A_0 asparagine is N267
350 (figure 6). These two interactions form the fundamental basis for recognizing the adenosine
351 pharmacophore and are invariant in all ADORs we have examined (see multiple sequence
352 alignments in supplementary figs. S12 and S13). In totality, nine amino acid residues in close
353 proximity to the adenosine analog in our shark A_0 homology model are highly conserved in all
354 known- and putative ADORs, including the ancestral branch (see also supplementary table S6).
355
356 **Discussion**
357 **Co-expression of shark A_0 and human CFTR**
358 We successfully co-expressed the shark A_0 adenosine receptor with human CFTR in
359 *Xenopus laevis* oocytes, which, to our knowledge, represents the first heterologous co-expression of
360 any adenosine receptor with CFTR in the literature. Oocytes appear to be an ideal system to
361 characterize shark A_0, since neither frog ADORs nor frog CFTR appears to be active or coupled.
362 We coupled an adenosine receptor from an elasmobranch shark, a subclass of Chondrichthyes fish
363 with a temporal range dating back to at least the Devonian period (~419-360 million years ago), to
364 human CFTR using the endogenous G-proteins and cellular enzymes of the oocyte. Other
365 investigators have in the past exploited CFTR for co-expression studies, specifically with alpha 2-
366 adrenergic-, beta 2-adrenergic-, delta-opioid-, and the 5HT1A receptors ((30), (31)), however those
367 receptors were mammalian in origin, which would not be viewed nearly as long-lived as receptors
368 identified in the shark. A_0 function in oocytes suggests that the interaction between receptors and
369 frog G-proteins is maintained despite the ancestral properties and structural differences A_0 has with

370 respect to more specialized ADORs. This highlights a likely conservation of the interface between
371 G-proteins and receptors with which they interact, across species and through evolution. Our results
372 also emphasize the versatility and value of the *Xenopus laevis* expression system for studies of
373 GPCR molecular evolution.
374
375 **A_0 exhibits unique ADOR pharmacology**
376 We characterized the shark A_0 receptor in *Xenopus* oocytes using a novel protocol, in
377 contrast to previous studies using binding assays, *in vivo* functional studies and cAMP
378 measurements. To this end it was necessary to couple the shark A_0 with a reporter target protein, in
379 this case human CFTR, to permit measurement of expression by electrophysiology. The data from
380 these studies revealed a unique profile for the shark A_0 receptor. Table 2 summarizes the
381 comparison of the A_0 receptor to other adenosine receptors with respect to agonist potency.
382 The shark A_0 differs: 1) from A_1 in its potency order of 2ClAdo and NECA, 2) from A_{2a}
383 and A_{2b} which have the reverse potency order and 3) from A_3 in which the least potent shark A_0
384 agonist, NECA, and the most potent shark A_0 agonist, R-PIA, have equal potencies. Therefore, the
385 shark A_0 appears to have a unique agonist profile judging from the potency order of R-PIA >
386 2ClAdo > NECA.
387 Subsequent qualitative studies further established the unique nature of the shark A_0. Table 3
388 compares the pharmacological profile for the shark A_0 to mammalian A_1, A_{2a}, A_{2b} and A_3
389 adenosine receptor subtypes. Analysis reveals the A_1 specific agonist R-PIA is the most potent in
390 the shark, however the A_1 selective agonist CPA is of intermediate potency. While S-PIA and
391 CGS21680 are more potent in the shark A_0 than in the A_1 receptors. All of the above are
392 inconsistent with an A_1-like receptor profile for A_0.
393 The shark A_0 receptor is unlike A_{2a} or A_{2b} due to its low potency of NECA - an A_2
394 selective agonist. Furthermore, selectivity of A_0 for S-PIA was unexpectedly high considering that
395 S-PIA is not relatively potent at A_1, A_{2a} or A_{2b} receptors. Interestingly, the A_{2a} specific agonist
396 CGS21680 has relatively high potency in the shark A_0 profile, while CV1808, also A_{2a} specific,
397 has a much lower potency in the profile. The shark A_0 profile bears little resemblance to that of
398 A_{2b} receptors especially with respect to the position of CGS21680, NECA, R-PIA and S-PIA.
399 Therefore, the shark A_0 resembles neither the A_{2a} nor the A_{2b} adenosine receptors (table 3).
400 Similarly, it is quite different from the known A_3 adenosine receptor profiles (table 3), with low
401 potency of NECA (intermediate potency in A_3), relatively high potency of CGS21680 and 5-PIA
402 (lower in the profile for A_3) and the large difference in potency of R-PIA and NECA, which are of
403 equal potency in the A_3 adenosine receptor profiles.
404 A comparison of the antagonist profiles yields similar results. Although the shark A_0
405 antagonist profile is reminiscent of the A_1 antagonist functional profile (table 3), when compared to
406 binding studies for the rat A_1 (supplementary table S7), the low potency of CGS15943 in the shark
407 A_0 profile is striking. The relative potency of CGS15943 is also incongruent with the rat A_{2a} and
408 rat A_{2b} profiles (supplementary table S8). Moreover, the potency order of DPCPX>PDl15199 in
409 the shark A_0, is reversed for A_{2a} receptors and A_{2b} receptors. It is clear that shark A_0 also possess
410 a unique antagonist profile.
411 In summary the agonist- and antagonist- profiles do not allow the classification of this
412 receptor into any known receptor subtype, providing functional evidence that A_0 is a unique
413 ADOR.
414

415 **A_0 is an extant ADOR ancestor**

416 Since the initial characterization of specialized adenosine receptor (ADOR) subtypes ~40
417 years ago, hundreds of ADORs have been identified. Many examples arise from genomic
418 sequencing but have not been characterized structurally or functionally. Phylogenetic analysis
419 shows that examples of specialized ADORs (i.e. A_1, A_{2a}, A_{2b} and A_3) are apparent throughout the
420 animal kingdom, including fish, amphibians, reptiles, birds and mammals. However, a separate
421 phylogenetic branch emerges from the analysis that contains ADORs in reptiles, amphibians and
422 fish, including the shark A_0 ADOR we have characterized here. Shark A_0, and the related
423 members on the branch, appear to be ancestral in nature. We draw this conclusion based on the
424 following: 1) amino acid sequence similarity of A_0 is roughly equally different from any specific
425 specialized subtype (A_1, A_{2a}, A_{2b} and A_3; see supplementary table S9); 2) the pharmacological
426 profile of A_0 is significantly different from the profiles of any subtype; 3) A_0 belongs to a
427 phylogenetic branch that is distinct from the branches formed by the other specialized subtypes;
428 and 4) ADOR members of the ancestor branch contains structural features unique only to
429 themselves, such as a minimal ECL2.

430 A_1, A_{2a}, A_{2b} and A_3 appear to be specialized for several reasons: 1) they have distinct and
431 consistent pharmacological profiles amongst their respective sub-branches; 2) they prefer to couple
432 to one G-protein alpha subunit (e.g. inhibitory $G_i\alpha$ or stimulatory $G_s\alpha$ on adenylate cyclase
433 activity), and 3) they are abundant in birds and mammals which are thought to arrive later in
434 evolution. The latter point highlights an interesting observation: specialized ADORs are prevalent
435 in mammals which arrived more recently in evolution time-scales, but the ancestral receptors,
436 including olfactory- and non-olfactory ADORs, appear to have been lost in mammals.
437

438 **Conclusion**

439 We have cloned, expressed and characterized an adenosine receptor (A_0) from the dogfish
440 shark (*Squalus acanthias*) that exhibits novel pharmacology compared to all known subtypes (A_1,
441 A_{2a}, A_{2b} and A_3). A_0 and its closest relatives form a distinct ancestral phylogenetic branch from
442 the known subtypes and do not appear have representation in birds or mammals. All ancestral
443 ADORs appear to have distinguishing structural elements, such as a minimally short extracellular
444 loop 2. Shark A_0 expression is strong in rectal gland where it likely regulates chloride secretion but
445 its expression is weak in brain, allowing us to conclude that is not olfactory in primary function. A
446 non-olfactory ancestral branch of ADORs, including A_0 from elasmobranchs, amphibians, and
447 reptiles is now apparent from the wealth of genomic sequencing data.

448 In contrast to the recently identified olfactory ADOR (A2c) found exclusively in fish (13),
449 A_0 was cloned from the shark rectal gland, a non-olfactory epithelial organ known for diverse
450 GPCR-mediated regulation of chloride secretion via the CFTR chloride channel (32). Shark CFTR
451 is more than 70% identical to human CFTR, and ADOR regulation of CFTR in sharks and
452 mammals is well described (33,34). Taken together, a long-standing evolutionary functional
453 coupling between ADORs and CFTR-mediated chloride secretion in epithelial tissues is evident,
454 and the elasmobranch A_0 receptor emerges as a non-olfactory extant ancestor of specialized ADOR
455 subtypes that most likely regulates CFTR in the shark.
456
457

Acknowledgements

We wish to thank Drs. Stephanie Halene and Kristina Lübbe for their important contributions toward the manuscript. This work was supported by a Howard Hughes Medical Institute Grant to SB, internal UAB funding to SGA, and by NIH grants R01 DK034208, NIEHS P30 ES003828 and NSF grant DBI-0453391 to JNF.

Data Availability

We agree to deposit the shark adenosine receptor nucleotide sequence to public repositories (NCBI) or make it available upon request.

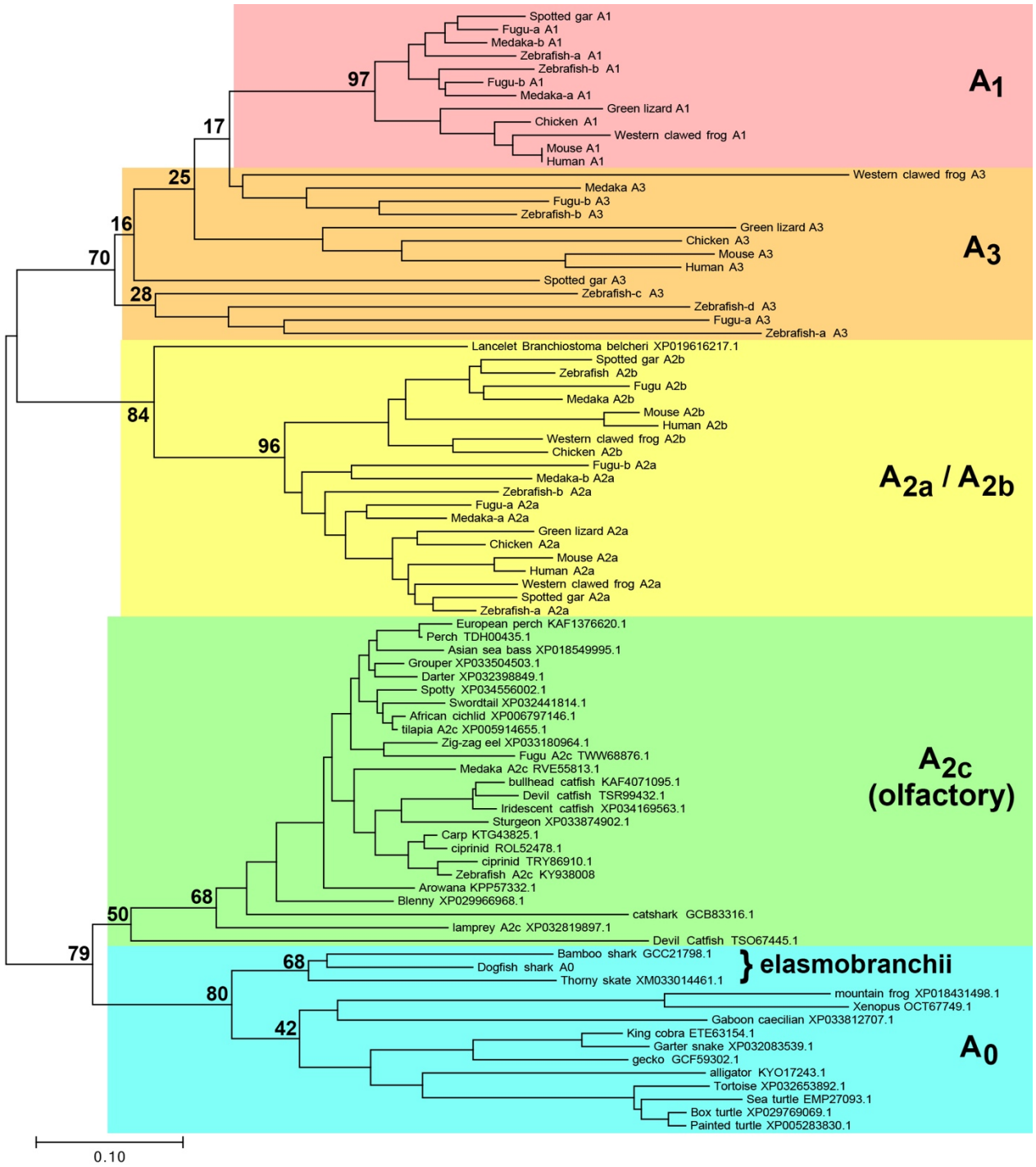

Figure 1. Phylogenetic relationships of ADOR taxa. Evolutionary history is inferred using the Neighbor-Joining method (35). The optimal tree is drawn to scale, with branch lengths in the same units as those of the evolutionary distances used to infer the tree. Distances were calculated using the Poisson correction method (36) and are in the units of the number of amino acids substitutions per site. A_1, A_{2a}, A_{2b}, A_3 and olfactory (A_{2c}) ADORs shown in Wakisaka, et al. 2017 are shown using the same names as in the paper. The first characterized A2c (Zebrafish, KY938008) by Wakisaka et al. is also shown in the figure. Additional putative ADORs found in this work are shown by species and Accession. The percentage of replicate trees in which the associated taxa clustered together in the bootstrap test using 500 replicates (Felsenstein 1985) are shown at selected branchpoints. Analyses were conducted using MEGA7 (Kumar, et al, 2016) using only full-length sequences for all receptors.

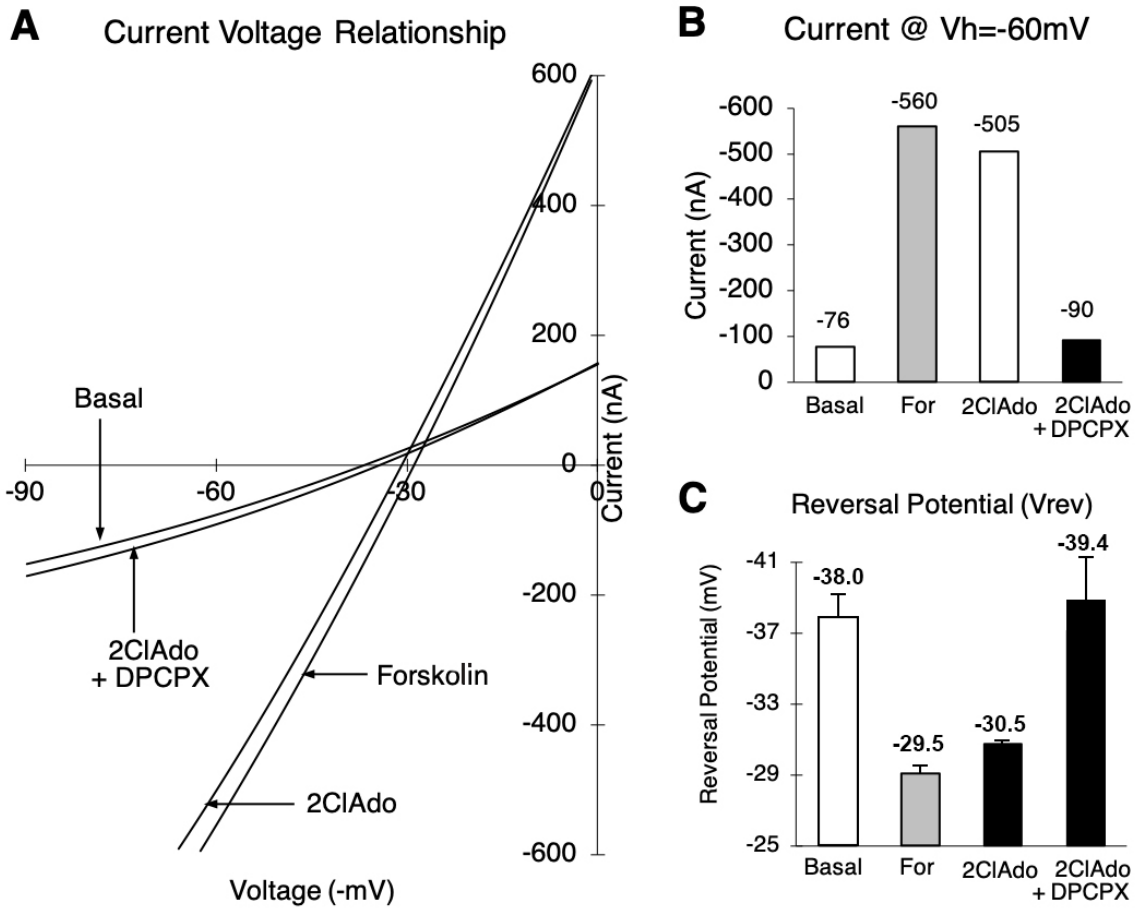

Figure 2. Current-Voltage (I-V) relationship illustrating the effects of forskolin, 2-chloroadenosine (a non-hydrolyzable form of adenosine) and 2-chloroadenosine & DPCPX (a known adenosine receptor antagonist) in a representative oocyte co-expressing the shark A_0 receptor and human CFTR Cl^- channel.

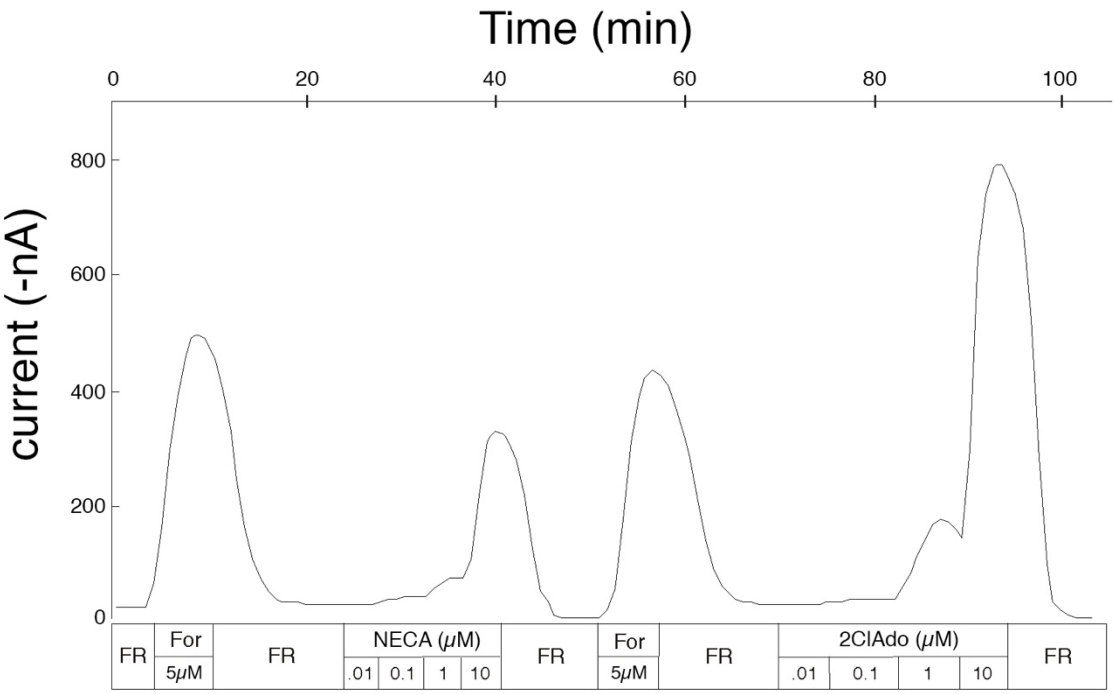

Figure 3. Representative tracing for the determination of the dose response profile for the shark A_0 adenosine receptor. A total of four oocytes were used for the determination of the dose response reported in the main text. Three oocytes, including results from one representative shown in the figure, were exposed to incremental doses of NECA, 2-chloroadenosine and R-PIA (not shown in the figure), while the fourth was used for the study of R-PIA exclusively.

492
493

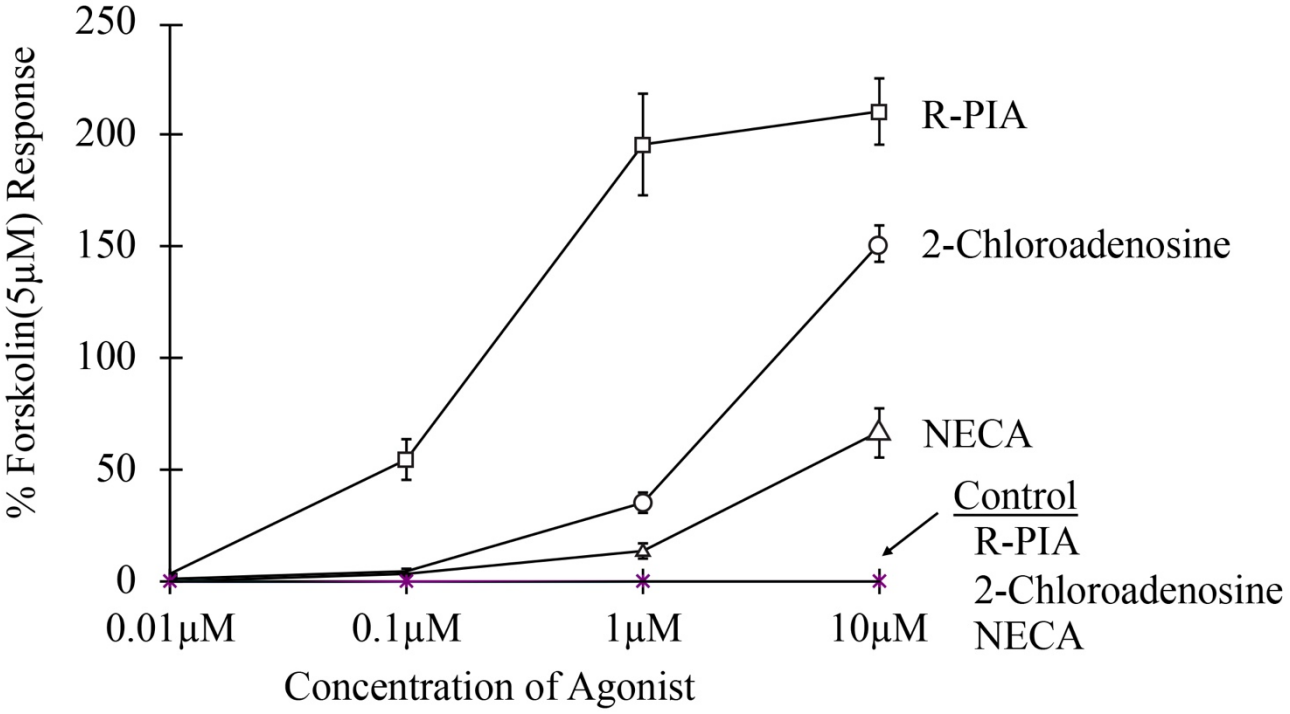

494

495 **Figure 4**. Dose response of the shark A_0 adenosine receptor in both A_0- and CFTR- co-injected oocytes as
496 well as CFTR only-injected oocytes (labeled "Control" in the figure). The controls were conducted in three
497 oocytes, with each agonist tested in each of the three oocytes (see asterisks (*) on the x-axis). The experimental
498 group was tested in four oocytes (NECA, n=3; 2-chloroadenosine, n=3; R-PIA, n=6; and are highlighted in
499 open squares, open triangles and open triangles, respectively).

500

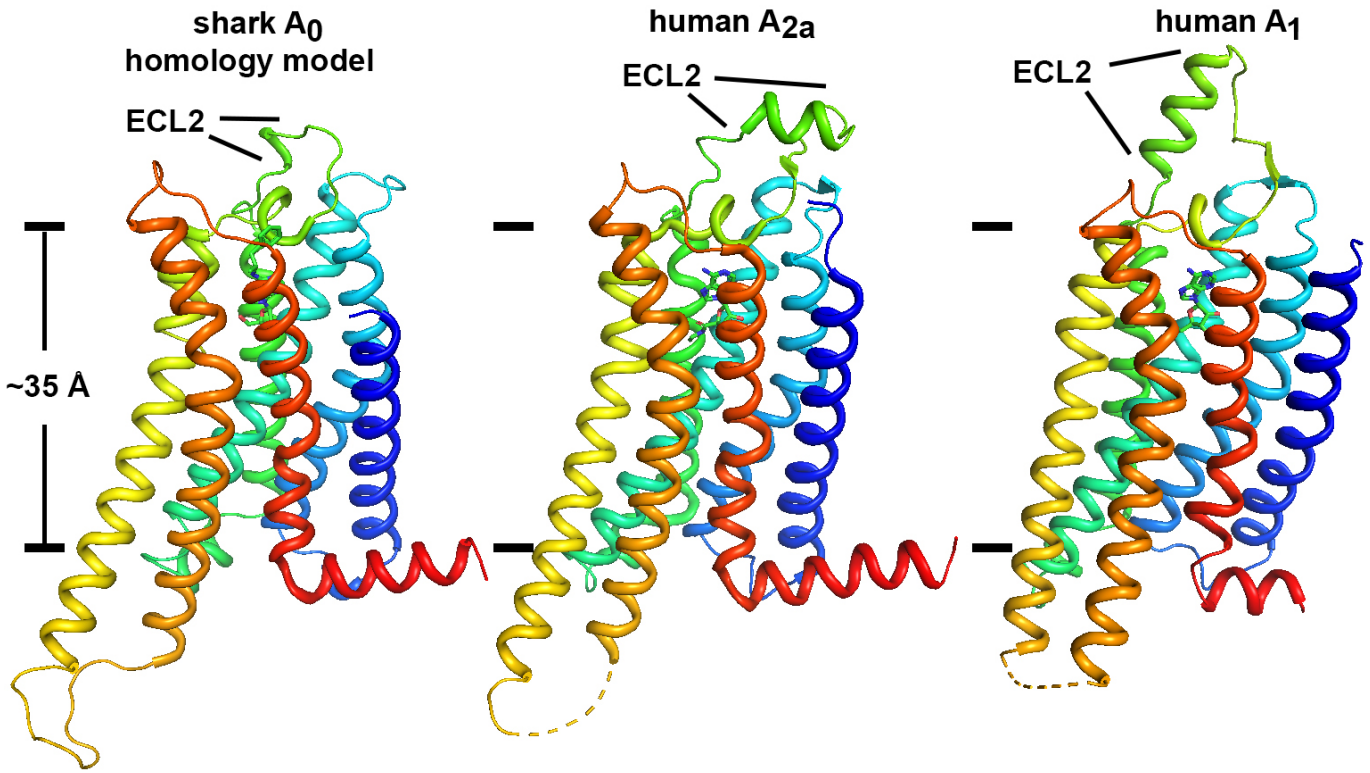

Figure 5. Overall view of the shark A_0 homology model compared to human A_{2a} and A_1 receptors (PDB codes 2ydv and 6d9h). The approximate position of the hydrophobic stretch of the lipid bilayer is depicted with lines separated by ~ 35 Å using conserved aromatic side chains as fiducials (27). A striking feature of shark A_0 compared to the more specialized ADORs is an abbreviated extracellular loop 2 (ECL2, labeled) and the relatively low profile that the A_0 receptor presents to the extracellular milieu. Multiple sequence alignment of all known- and putative receptor orthologs (supplementary figs. S9 and S10) reveals that an abbreviated ECL2 appears to be unique feature of ancestral ADORs.

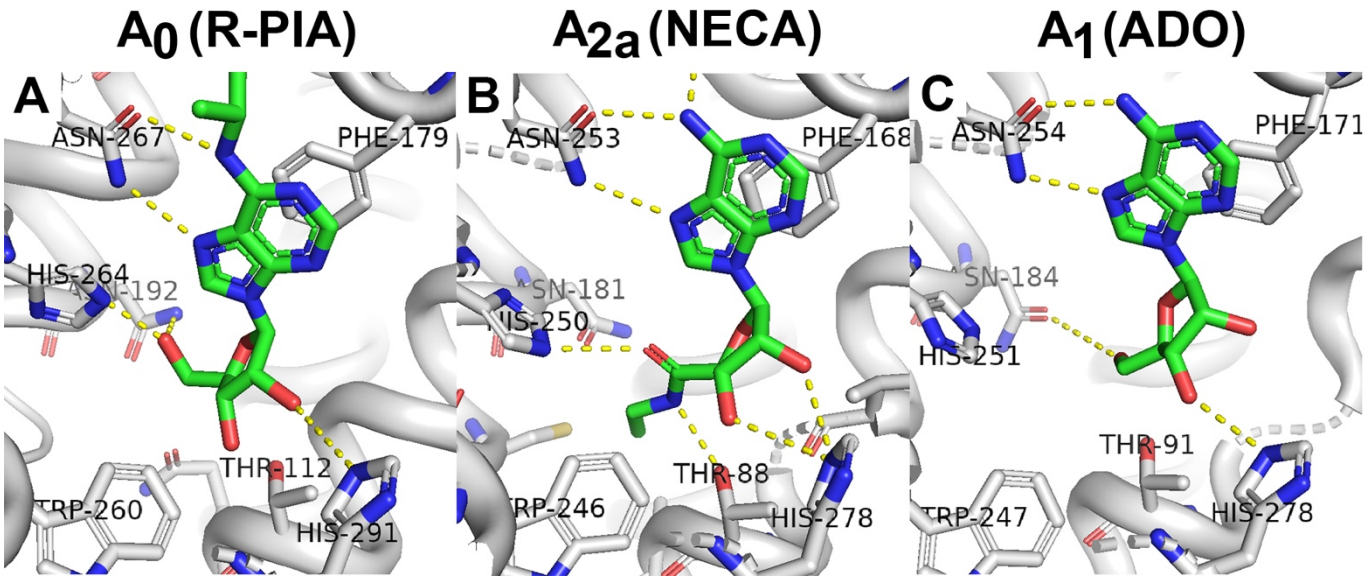

Figure 6. Binding pockets for adenosine and adenosine agonists. Panel A shows a potential binding mode of R-phenyl-isopropyl adenosine (R-PIA) as it appears in our refined homology model of the shark A_0 receptor. The purpose is not to highlight precise interactions, bonds or geometry, but to indicate that the major known adenosine-binding ligands are conserved in the shark A_0 ancestor receptor and are well positioned to potentially interact with ligands. For comparison, the location of N-ethyl-carboxyl adenosine (NECA) binding in the 2.6 Å x-ray structure of human A_{2a} receptor (PDB code 2ydv) is shown in panel B. Panel C shows the location of adenosine (ADO) binding in the 3.6 Å cryo-EM structure of the human A_1 receptor (PDB code 6d9h).

524

A_1 agonist	CPA>R-PIA=NECA>2ClAdo>S-PIA>DPMA>CV1808>CGS21680
A_{2b} agonist	NECA>R-PIA>2ClAdo>CPA>DPMA>S-PIA>CV1808>CGS21680
A_{2b} antagonist	8PT>PD115199>DPCPX>CGS15943>CSC

525
526 **Table 1.** Pharmacological Profiles of Human Adenosine Receptors in *Xenopus* oocytes obtained from
527 this study.
528
529
530
531
532

533
534

Receptor subtype	Potency order
Shark A_0	R-PIA>2ClAdo>NECA
A_1	R-PIA>NECA>2ClAdo
A_{2a}	NECA>2ClAdo>R-PIA
A_{2b}	NECA>2ClAdo>R-PIA
A_3	R-PIA≈NECA

535
536 **Table 2.** Summary of agonist potency order of shark A_0 determined from this study compared to potencies
537 for A_1, A_{2a}, A_{2b} and A_3 receptors from binding/functional studies in the literature. See expanded
538 supplementary tables S7 and S8, including references.
539
540
541

542

Subtype	Ag/Ant	Functional Profiles*
A_0	Ag.	R-PIA>S-PIA>CGS21680>CPA>2ClAdo>CV1808≥DPMA>NECA
	Antag.	DPCPX>PD115199>8PT>CSC>CGS15943
A_1	Ag.	CPA>R-PIA=CHA≥NECA>2ClAdo>S-PIA>CV1808≥CGS21680
	Antag.	DPCPX>PD115199>8PT
A_{2a}	Ag.	CGS21680=NECA>CV1808≥2ClAdo>R-PIA=CHA=CPA>S-PIA
	Antag.	PD115199>DPCPX=8PT
A_{2b}	Ag.	NECA>2ClAdo>R-PIA=CHA>S-PIA≥CV1808≥CGS21680
	Antag.	DPCPX=8PT≥PD115199
A_3	Ag.	APNEA>R-PIA=NECA>CGS21680
	Antag.	None identified in this review

543 *Data adapted from Collis et.al. Adenosine receptor subtypes. TiPS. Oct. 1993(Vol 14)

544

545 **Table 3.** Comparison of data from qualitative studies of the shark A_0 in *Xenopus* oocytes and functional
546 studies of the adenosine A_1, A_{2a}, A_{2b} and A_3 receptor subtype from the literature. See expanded
547 supplementary tables S7 and S8, including references.

548

549

550

551 **References**

552 1. Burnstock, G. (1978) *A basis for distinguishing two types of purinergic receptor.*, Raven Press,
553 New York
554 2. Olah, M. E. (1997) Identification of A2a adenosine receptor domains involved in selective
555 coupling to Gs. Analysis of chimeric A1/A2a adenosine receptors. *J Biol Chem* **272**, 337-344
556 3. Sweeney, M. I., and Dolphin, A. C. (1995) Adenosine A1 agonists and the Ca2+ channel agonist
557 bay K 8644 produce a synergistic stimulation of the GTPase activity of Go in rat frontal cortical
558 membranes. *J Neurochem* **64**, 2034-2042
559 4. Palmer, T. M., and Stiles, G. L. (1995) Adenosine receptors. *Neuropharmacology* **34**, 683-694
560 5. Jockers, R., Linder, M. E., Hohenegger, M., Nanoff, C., Bertin, B., Strosberg, A. D., Marullo, S.,
561 and Freissmuth, M. (1994) Species difference in the G protein selectivity of the human and
562 bovine A1-adenosine receptor. *J Biol Chem* **269**, 32077-32084
563 6. Marala, R. B., and Mustafa, S. J. (1993) Direct evidence for the coupling of A2-adenosine
564 receptor to stimulatory guanine nucleotide-binding-protein in bovine brain striatum. *J*
565 *Pharmacol Exp Ther* **266**, 294-300
566 7. Freholm, B. B. e. a. (1994) Nomenclature and Classification of Purinoceptors. *Pharmacological*
567 *Reviews* **46**, 143-156
568 8. Burns, R. F., Lu, G. H., and Pugsley, T. A. (1987) Adenosine Receptor Subtypes: Binding Studies.
569 in *Topics and Prespectives in Adenosine Research*, Springer-Verlag, Berlin, Heidelberg. pp 59-73
570 9. Kelley, G., Aassar, O., and Forrest, J. J. (1991) Endogenous adenosine is an autocoid feedback
571 inhibitor f chloride transport in the shark rectal gland. *Journal of clinical investigation* **88**, 1933-
572 1939
573 10. Forrest, J. N. J. (1996) Cellular and molecular biology of chloride secretion in the shark rectal
574 gland: regulation by adenosine receptors. [Review]. *Kidney International* **49(6)**, 1557-1562
575 11. Forrest, J. N., Jr., Aller, S. G., Wood, S. J., Ratner, M. A., Forrest, J. K., and Kelley, G. G. (1997)
576 Cadmium disrupts the signal transduction pathway of both inhibitory and stimulatory receptors
577 regulating chloride secretion in the shark rectal gland. *J Exp Zool* **279**, 530-536
578 12. Marshall, J., Martin, K., Picciotto, M., HOCkfield, S., Nairn, A., and Kaczmarek, L. (1991)
579 Identification and localization of a dogfish homolog of human cyctic fibrosis transmembrance
580 conductance regulator. *The journal of biological chemistry* **266**, 22749-22754
581 13. Wakisaka, N., Miyasaka, N., Koide, T., Masuda, M., Hiraki-Kajiyama, T., and Yoshihara, Y. (2017)
582 An Adenosine Receptor for Olfaction in Fish. *Curr Biol* **27**, 1437-1447 e1434
583 14. Thompson, J. D., Higgins, D. G., and Gibson, T. J. (1994) CLUSTAL W: improving the sensitivity of
584 progressive multiple sequence alignment through sequence weighting, position-specific gap
585 penalties and weight matrix choice. *Nucleic Acids Res* **22**, 4673-4680
586 15. Madeira, F., Park, Y. M., Lee, J., Buso, N., Gur, T., Madhusoodanan, N., Basutkar, P., Tivey, A. R.
587 N., Potter, S. C., Finn, R. D., and Lopez, R. (2019) The EMBL-EBI search and sequence analysis
588 tools APIs in 2019. *Nucleic Acids Res* **47**, W636-W641
589 16. Rice, P., Longden, I., and Bleasby, A. (2000) EMBOSS: the European Molecular Biology Open
590 Software Suite. *Trends Genet* **16**, 276-277
591 17. Nordstrom, K. J., Sallman Almen, M., Edstam, M. M., Fredriksson, R., and Schioth, H. B. (2011)
592 Independent HHsearch, Needleman--Wunsch-based, and motif analyses reveal the overall
593 hierarchy for most of the G protein-coupled receptor families. *Mol Biol Evol* **28**, 2471-2480
594 18. Kumar, S., Stecher, G., and Tamura, K. (2016) MEGA7: Molecular Evolutionary Genetics Analysis
595 Version 7.0 for Bigger Datasets. *Mol Biol Evol* **33**, 1870-1874

596 19. Lebon, G., Warne, T., Edwards, P. C., Bennett, K., Langmead, C. J., Leslie, A. G., and Tate, C. G.
597 (2011) Agonist-bound adenosine A2A receptor structures reveal common features of GPCR
598 activation. *Nature* **474**, 521-525
599 20. Draper-Joyce, C. J., Khoshouei, M., Thal, D. M., Liang, Y. L., Nguyen, A. T. N., Furness, S. G. B.,
600 Venugopal, H., Baltos, J. A., Plitzko, J. M., Danev, R., Baumeister, W., May, L. T., Wootten, D.,
601 Sexton, P. M., Glukhova, A., and Christopoulos, A. (2018) Structure of the adenosine-bound
602 human adenosine A1 receptor-Gi complex. *Nature* **558**, 559-563
603 21. Garcia-Nafria, J., Lee, Y., Bai, X., Carpenter, B., and Tate, C. G. (2018) Cryo-EM structure of the
604 adenosine A2A receptor coupled to an engineered heterotrimeric G protein. *Elife* **7**
605 22. Lebon, G., Edwards, P. C., Leslie, A. G., and Tate, C. G. (2015) Molecular Determinants of
606 CGS21680 Binding to the Human Adenosine A2A Receptor. *Mol Pharmacol* **87**, 907-915
607 23. Sayers, E. (2017) Database Resources of the National Center for biotechnology Information.
608 *Nucleic Acids Res* **45**, D12-D17
609 24. Emsley, P., Lohkamp, B., Scott, W. G., and Cowtan, K. (2010) Features and development of Coot.
610 *Acta Crystallogr D Biol Crystallogr* **66**, 486-501
611 25. Adams, P. D., Afonine, P. V., Bunkoczi, G., Chen, V. B., Davis, I. W., Echols, N., Headd, J. J., Hung,
612 L. W., Kapral, G. J., Grosse-Kunstleve, R. W., McCoy, A. J., Moriarty, N. W., Oeffner, R., Read, R.
613 J., Richardson, D. C., Richardson, J. S., Terwilliger, T. C., and Zwart, P. H. (2010) PHENIX: a
614 comprehensive Python-based system for macromolecular structure solution. *Acta Crystallogr D*
615 *Biol Crystallogr* **66**, 213-221
616 26. Weininger, D. (1988) SMILES, a chemical language and information system. *J Chem Inform*
617 *Computer Sci* **28**, 31-36
618 27. de Planque, M. R., Kruijtzer, J. A., Liskamp, R. M., Marsh, D., Greathouse, D. V., Koeppe, R. E.,
619 2nd, de Kruijff, B., and Killian, J. A. (1999) Different membrane anchoring positions of
620 tryptophan and lysine in synthetic transmembrane alpha-helical peptides. *J Biol Chem* **274**,
621 20839-20846
622 28. Devor, D. C., Forrest, J. N., Jr., Suggs, W. K., and Frizzell, R. A. (1995) cAMP-activated Cl-
623 channels in primary cultures of spiny dogfish (Squalus acanthias) rectal gland. *Am J Physiol* **268**,
624 C70-79
625 29. Xu, F., Wu, H., Katritch, V., Han, G. W., Jacobson, K. A., Gao, Z. G., Cherezov, V., and Stevens, R.
626 C. (2011) Structure of an agonist-bound human A2A adenosine receptor. *Science* **332**, 322-327
627 30. Birnbaum, A. K., Wotta, D. R., Law, P. Y., and Wilcox, G. L. (1995) Functional expression of
628 adrenergic and opioid receptors in Xenopus oocytes: interaction between alpha 2- and beta 2-
629 adrenergic receptors. *Brain Res Mol Brain Res* **28**, 72-80
630 31. Uezono, Y., Bradley, J., Min, C., McCarty, N. A., Quick, M., Riordan, J. R., Chavkin, C., Zinn, K.,
631 Lester, H. A., and Davidson, N. (1993) Receptors that couple to 2 classes of G proteins increase
632 cAMP and activate CFTR expressed in Xenopus oocytes. *Receptors Channels* **1**, 233-241
633 32. Forrest, J. N., Jr. (2016) The Shark Rectal Gland Model: A Champion of Receptor Mediated
634 Chloride Secretion through Cftr. *Trans Am Clin Climatol Assoc* **127**, 162-175
635 33. Clancy, J. P., Ruiz, F. E., and Sorscher, E. J. (1999) Adenosine and its nucleotides activate wild-
636 type and R117H CFTR through an A2B receptor-coupled pathway. *Am J Physiol* **276**, C361-369
637 34. Kelley, G. G., Poeschla, E. M., Barron, H. V., and Forrest, J. N., Jr. (1990) A1 adenosine receptors
638 inhibit chloride transport in the shark rectal gland. Dissociation of inhibition and cyclic AMP. *J*
639 *Clin Invest* **85**, 1629-1636
640 35. Saitou, N., and Nei, M. (1987) The neighbor-joining method: a new method for reconstructing
641 phylogenetic trees. *Mol Biol Evol* **4**, 406-425

642 36. Zuckerkandl, E. a. P., L. (1965) Evolutionary divergence and convergence in proteins. in *Evolving*
643 *Genes and Proteins*, Academic Press, New York. pp 97-166
644